Vol. 516 No. 8   29 February 2008   ISSN 0040-6090

ELSEVIER

thin solid films

International Journal on the Science and Technology of Condensed Matter Films

Available online at

ScienceDirect

www.sciencedirect.com

http://www.elsevier.com/locate/tsf

Editor-in-Chief:
J.E. Greene

Use of surface plasmon-coupled emission for enhancing light transmission through Top-Emitting Organic Light Emitting Diodes

Xiaodong Wu [a], Mustafa H. Chowdhury [b], Chris D. Geddes [b,c,*], Kadir Aslan [c],
Roman Domszy [a], Joseph R. Lakowicz [b], Arthur J.-M. Yang [a,*]

[a] *Industrial Science and Technology Network Inc., 2101 Pennsylvania Avenue, York, PA, 17404, USA*
[b] *Center for Fluorescence Spectroscopy, Medical Biotechnology Center, University of Maryland School of Medicine,
725 West Lombard Street, Baltimore, MD, 21201, USA*
[c] *Institute of Fluorescence, Laboratory for Advanced Medical Plasmonics, Medical Biotechnology Center,
University of Maryland Biotechnology Institute, 725 West Lombard Street, Baltimore, MD, 21201, USA*

Abstract

In this paper, we perform surface plasmon-coupled emission studies on Rhodamine 6G molecules embedded in a corrugated structure of a thin film composed of fluorinated silica particles, and a binding medium. Our results show enhancements of photoluminescence due to surface corrugation. By varying the size of the fluorinated silica nanoparticles we were able to control the surface correlation length scale of the corrugated surface structure. It was found that the coupling efficiency of the directional light emission is strongly correlated to the surface morphology, particularly the surface correlation length, of the corrugated dielectric structure. This substantial enhancement of signal could potentially be utilized in Organic Light Emitting Diode devices to enhance the light emission and transmission through a thin silver layer which can also serve as the cathode in Top-Emitting Organic Light Emitting Diodes.
© 2007 Elsevier B.V. All rights reserved.

1. Introduction

Replacing relatively heavy Cathode Ray Tube monitors with portable and light flat panels has become the major trend in the whole display industry. This is primarily due to the rapid growth in demand for hand-held communication devices such as mobile phones, palm pilots and portable computing equipment, which require flat displaying devices that are light, thin and power efficient. Consequently, the flat displaying technology is expected to advance substantially in the coming decades. Three displaying technologies such as field emission, Organic Light Emitting Diodes (OLED) and Liquid Crystal Displays (LCD) are likely to be dominant in the future optical displaying market. There is unique opportunity for the application of nanotechnology to advance the underlying light emission and optical wave guiding techniques in such devices. This is likely to revolutionize future designs of display panels. We believe that innovations in this field will be eventually accomplished predominantly with the advancements in metallic nanotechnology.

In the past few decades, the solid-state technology revolution in electronics, showcased by precise fabrication of semiconductors and semimetals, has led to maneuvering electron transfers among molecular orbital groups. The developments of Light Emitting Diodes (LED) and OLEDs demonstrated that these molecularly engineered composites could successfully generate electromagnetic (EM) waves at a precise visible spectrum range (i.e. light emission at a desired frequency range). In addition, the recent discovery of surface plasmon-coupled emission (SPCE) proved that nanometer sized metallic thin films (30–50 nm thickness),

---

* Corresponding authors. Geddes is to be contacted at Institute of Fluorescence, Laboratory for Advanced Medical Plasmonics, Medical Biotechnology Center, University of Maryland Biotechnology Institute, 725 West Lombard Street, Baltimore, MD, 21201, USA. Tel.: +1 410 706 3149; fax: +1 410 706 4600. Yang, Fax: +1 717 843 0705.

E-mail addresses: geddes@umbi.umd.edu (C.D. Geddes),
ajyang@istninc.com (A.J.-M. Yang).

when located in the near field (100–200 nm) of an LED or OLED emitting source, could substantially enhance the quantum yield and the radiation output of such a device [1,2]. Such developments in generating and guiding EM waves at the optical frequencies have clearly mapped out a technical direction for future applications of metallic nanotechnology in the advancement of optical displaying technologies.

OLEDs are being commercially exploited due to the variety of appealing features that they possess such as their ease of fabrication [3–5]. Conventional OLEDs are typically substrate emitting (where light is emitted through a glass substrate). For the different kinds of display applications mentioned above, active matrix driven panels are required, and this can be achieved through top-emitting OLEDs, where the emission takes place through the cathodes (instead of the glass substrate) [3–5]. This allows the OLED to be incorporated into silicon substrates and hence facilitating the "on-chip" integration of light emitting and control components with silicon "driver" electronics. This is an advantage since a device capable of emitting light from the top cathode would allow all circuitry components such as wiring and transistors to be placed at the bottom, hence avoiding interference with the light output. Therefore, there has been an increasing demand in Top-Emitting Light Emitting Diodes (TOLED) for active-matrix OLED displays. Fig. 1 shows a schematic of a generic TOLED and a Substrate-Emitting Light Emitting Diode.

Achieving high efficiency of performance for OLEDs involves consideration of two primary issues, namely the efficiency with which radiative excitons are formed, and the efficiency with which light resulting from the decay of these excitons is extracted as useful radiation [3–5]. E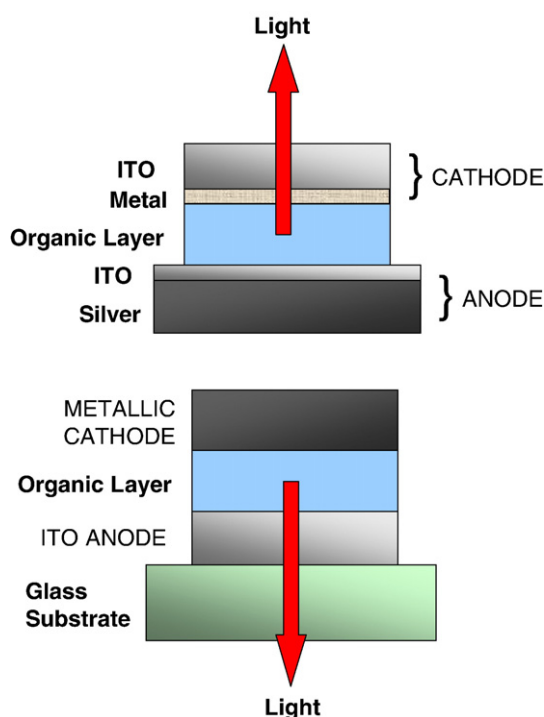xcitons are generated by the injection of charge carriers and it is the radiative decay of these excitons that produces light. The probability that an exciton decay within the organic layer of an OLED will lead to an emitted photon is reduced by coupling of the exciton to bound optical modes such as waveguide and surface plasmon-polaritron (SPP) modes that are supported by the substrate, or lost as heat to one of the electrodes [3–5]. It has been reported that OLED efficiency can be significantly improved by introducing methods to couple the bounded optical modes to useful far-field radiation. One way for achieving this is by introducing a periodic structure of wavelength scale in the optically active layer of an OLED which allows the waveguide modes normally trapped in the substrate to be Bragg scattered out of the structure [3–6]. Other ways of increasing efficiency is by scattering off random microstructures and through refractive index control [4,7–9].

We have published several reports over the last several years where we describe the use of metallic surfaces and sub-wavelength sized metallic nanoparticles to modify the far-field emissive properties of optically excited fluorophores [10–15]. We reported that under appropriate conditions, close proximity fluorophores (in the near-field) to silver nanoparticles can lead to increased system quantum yields, increased photostability and decreased lifetimes [15]. We explained these effects of metals on fluorescence, using a simple concept based on the ability of fluorophore-induced plasmons to radiate away from the metal surface. We refer to this concept as the radiating plasmon model [16,17]. Our studies on fluorophore–metal interactions have led us to demonstrate that resonance interactions can occur between excited fluorophores in close proximity (in the near-field) to thin *continuous films* of metal attached to glass prisms, resulting in the excitation of surface plasmons in the metal, and the highly directional emission (in the far-field) by the plasmons into the glass side that appear to be with the same spectral distribution as the fluorophore. We termed this phenomenon as SPCE, which is in fact related to Surface Plasmon Resonance (SPR) [13,14,18–24]. SPR is the absorption of light by a thin metal film, usually gold or silver, when the wavevector of the *p*-polarized incident light matches the wavevector of the surface plasmons at the sample–metal interface [13,14,18–24]. This wavevector matching condition requires the light incident on the metal to pass through a prism of high refractive index, and does not occur if the light is directly incident on the metal through air. The angle of incidence through the prism needs to be adjusted to match the wavevector and hence resonantly excite the surface plasmons [13,14,18–24]. This angle is called the SPR angle for the incident wavelength (θ_{SP}). The reflectivity of the metal film is high except for a small range of angles around θ_{SP} [13,14]. In SPCE, the emission is detected at a specific angle, θ_{SP}, rather than absorbed, where excited fluorophore dipoles near the metal couple to the surface plasmons [13,14,18–24]. This coupling results in the plasmons radiating at the fluorophore emission wavelength at sharply defined angles from the normal on the prism side of the setup. This angle is elegantly equal to the SPR angle for the emission wavelength [13,14,18–24]. We have shown that for fluorophores embedded in a polyvinyl alcohol (PVA) film less than 160 nm thick (i.e. fluorophores within 160 nm of the metal film), the SPCE occurs at a single angle in the glass substrate and displays only *p*-polarization [18]. As the PVA thickness increases to 300 nm,

Fig. 1. General schematic of a top-emitting OLED (top) and substrate-emitting OLED (bottom). ITO = Indium Tin Oxide.

Table 1
Ingredients for preparation of nanoparticles

Particle size nm	Isopropanol ml	TEOS ml	F-TEOS ml	Water ml	NH₄OH ml
150	20	1.4	0.6	1.5	1
330	20	1.4	0.6	2.92	1
482	20	2.8	0.85	2.0	1

we reported observing SPCE at two angles, with different s or p polarization for each angle [18]. In addition we have reported that for PVA films from 500 to 750 nm thick, SPCE is observed at three or four angles, with alternating s and p polarizations [18]. The multiple angles of SPCE and the unusual s-polarized emission were associated with waveguide modes in the metal–PVA composite film [18].

In this paper, we performed SPCE studies on laser-excited Rhodamine 6G (R6G) which was embedded within a corrugated dielectric mixture layer and spin-coated onto a 45 nm silver film. The coupling of fluorophore excitation to the silver film resulted in highly directional SPCE through both the silver and the glass substrate. By creating a corrugated structure within the film layer containing the dye molecules, we observed enhancements of photoluminescence due to surface corrugation. The dielectric mixture was composed of fluorinated silica particles and a binding medium. By varying the size of the fluorinated silica nanoparticles we were able to control the surface correlation length scale of the corrugated surface structure. It was found that the coupling efficiency of the directional light emission is strongly correlated to the surface morphology, particularly the surface correlation length, of the corrugated dielectric structure. The substantial enhancement of signal, as observed in this study, could potentially be utilized in OLED devices to enhance the light emission and transmission through a thin silver layer, which could potentially also serve as the top silver electrode in TOLEDs.

2. Materials and methods

2.1. Materials

Premium quality Aminopropyltriethoxy-silane (APS) coated glass slides (75×25 mm), silver wire (99.99+% purity), silicon monoxide pieces (99.99% purity) and R6G were obtained from Sigma-Aldrich (St. Louis, MO). Tetraethoxysilane (TEOS) and (tridecafluoro-1,1,2,2-tetrahydrooctyl)triethoxysilane (F-TEOS) were obtained from Gelest Inc. (Morrisville, PA) and used as received. Colloidal silica dispersed in isopropanol with average particle size 12 nm (IPA-ST) was obtained from Nissan Chemical (Houston, TX).

2.2. Formation of continuous thin films of silver on APS-coated glass substrates

Forty five nanometers of silver were deposited on separate APS-coated glass slides using an Edwards Auto 306 Vacuum Evaporation chamber (West Sussex, UK) under ultra high vacuum ($<4\times10^{-4}$ Pa). In each case, the metal deposition step

was followed by the deposition of 5 nm of silica via evaporation without breaking vacuum. This step served to protect the metal surface from oxidation.

2.3. Formation of roughened silica nanoparticle based sol–gel coating layer

Fluorinated silica nanoparticles with a controlled particle size (100–500 nm) were synthesized [25] using a modified version of the Stöber process [26,27]. The particle size is determined by the concentration of F-TEOS and water used in the reaction mixture. In a reaction vial and in the amounts indicated in Table 1, isopropanol, TEOS and F-TEOS were added and mixed with a magnetic stirrer at a high speed for 2 min at 25 °C. During the stirring, deionized water and 1 ml concentrated ammonium hydroxide solution (28% w/w) were added to the mixture. The mixture was stirred for another 30 min. The solution was allowed to age for two days. The nanoparticle size from this process was measured by light scattering (90-Plus Analyzer, Brookhaven Instruments Corporation).

A silica sol was prepared by vigorously stirring for 2 h a mixture of 10 ml isopropanol, 6 ml TEOS, 1.44 ml water and 1 ml hydrochloric acid (0.2 M). The silica sol was added to the silica nanoparticles (30 wt.% of the final coating mixture consisted of the silica sol). Sol–gel coatings embedded with silica nanoparticles in sizes of 12, 150, 330, 482 nm respectively were deposited on the surface by spin coating to create a randomly roughened surface. R6G was then deposited on the roughened surface by spin coating a 100 µM isopropanol solution at 1700 rpm. The
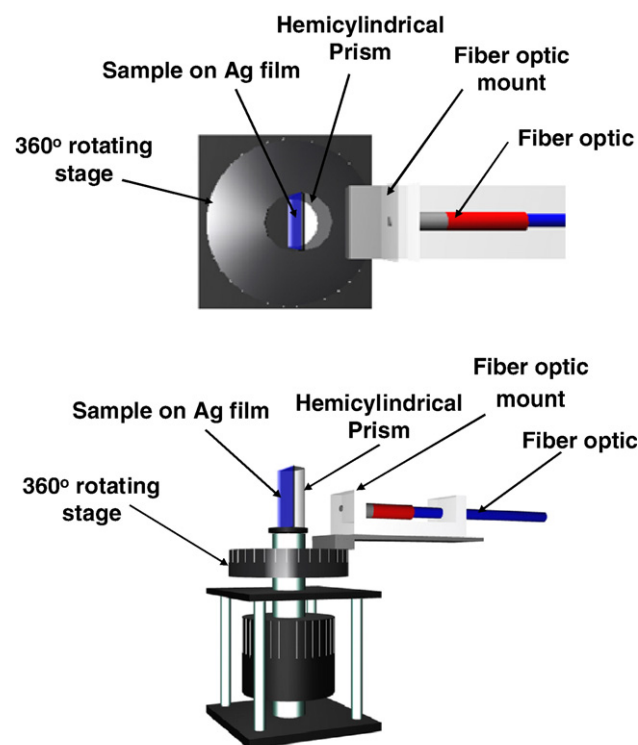

Fig. 2. Experimental geometry used for surface plasmon-coupled emission (SPCE). (top) — view from the top, (bottom) — side view.
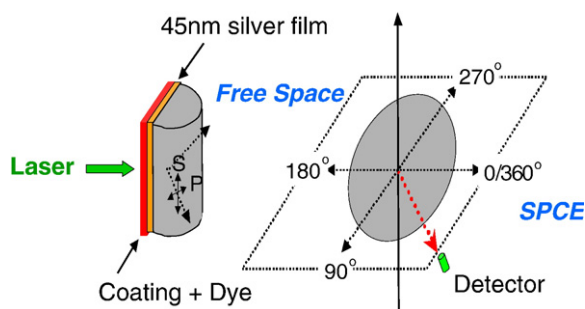
Fig. 3. Definition of angles for SPCE and free space.

rotatory stage. The sample was excited using a 532 nm laser in reverse Kretschmann configuration (RK) [13,14,18–24]. Both SPCE and free space spectra were collected using a model SD 2000 Ocean Optics spectrometer (Dunedin, FL) connected to the above mentioned optical fiber where a 570 nm Long Pass filter was used to filter out the excitation line. The spectra were collected with an integration time between 0.5 and 2 s (depending on the intensity of the SPCE signal). Both unpolarized, *p* and *s*-polarized signal information was collected for the SPCE signal and the free space signal. A pictorial representation of the top and side view of the setup is presented in Fig. 2.

3. Results and discussion

actual film thickness was measured using a Filmetrics F20 Thin Film Measurement System (San Diego, CA). The surface morphology of the sample was characterized by atomic force microscopy (AFM) using a Nanoscope IIIA AFM (Veeco Instruments, Woodbury, NY).

2.4. SPCE measurements

The metal-coated slides containing the various samples were attached to a hemicylindrical prism made with BK7 glass (*n* = 1.52) and the refractive index was matched using spectrophotometric grade glycerol (*n* = 1.475) between the back of the glass slide (uncoated side) and the prism. This unit was then placed on a precise 360° rotatory stage which was built in-house. The rotatory stage allowed the collection of light at all angles around the sample chamber. An Ocean Optics low OH 1000 μm diameter optical fiber with NA of 0.22 (Dunedin, FL) used for collecting the SPCE and free space emission was mounted on a holder, which was screwed on to the base of the

All the samples in this study were excited in the RK configuration, where the incident light cannot directly excite surface plasmons in the metal film. Hence the angle-dependent emission would be primarily due to the near-field interaction of metal surface plasmons with the excited fluorophores, not with the incident light. We measured the emission intensities for all accessible angles relative to the normal axis. The definition of angles for free space and SPCE in the experimental setup is illustrated in Fig. 3.

For sample A, illustrated in Fig. 4 (Top Left), which contains the smallest silica nanoparticles of 12 nm diameter, a film thickness of roughly 316 nm, and has the lowest surface roughness, there are two distinct SPCE peak angles at 314° (or 44° due to symmetry) and 288° (or 72° due to symmetry), respectively. According to previous literature results [18,24], those peaks can be attributed to waveguide modes, where both *s* (transverse electric) and *p* (transverse magnetic) modes are
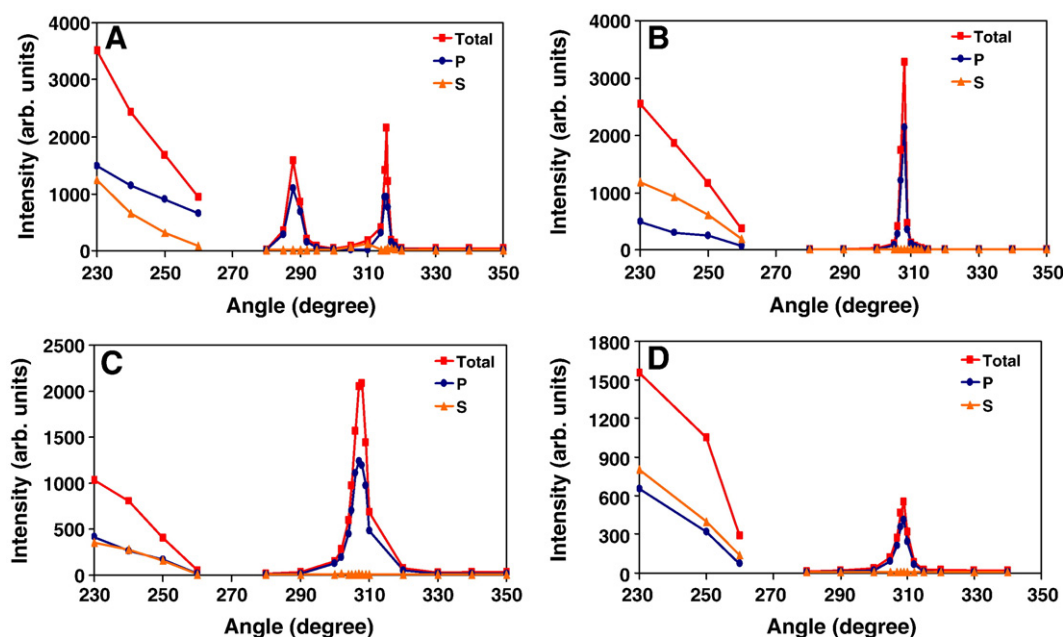

Fig. 4. (Top left) Angular distribution of SPCE for Sample A (coating thickness approx. 316 nm, consisting of 12 nm silica particles) Vs free space intensity (between 230° and 260°); (top right) sample B (coating thickness approx. 120 nm, consisting of 150 nm silica particles) Vs free space intensity (between 230° and 260°); (bottom left) sample C (coating thickness approx. 200–300 nm, consisting of 330 nm silica particles) Vs free space intensity (between 230° and 260°); (bottom right) sample D (coating thickness approx. 300 nm, consisting of 482 nm silica particles) Vs free space intensity (between 230° and 260°).
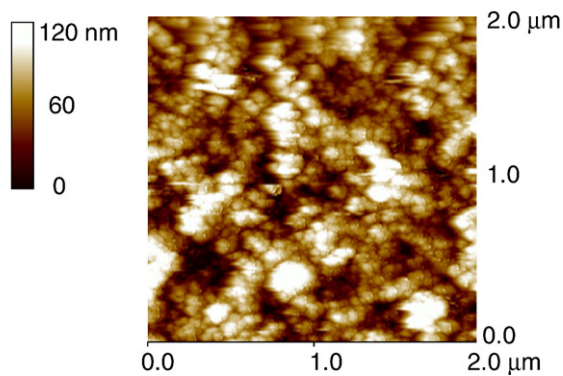
Fig. 5. AFM contour height image of sample B (150 nm silica particles).

known to propagate in a nonmetallic dielectric layer because the configuration supports propagating waves of either polarization. The far field fluorescence was also measured as free space intensity on the opposite of prism at the angles between 90° and 270°.

The results for sample B, where 150 nm silica nanoparticles were used and had an average thickness of approximately 120 nm, is found in Fig. 4 (Top Right). It can be seen that only one p-polarized emission peak was observed at 308° (or 52°). The intensity of the SPCE was compared with the free space intensity at 230°. The ratio is found to be 1.3. The results for sample C, where 330 nm silica nanoparticles were used and had an average film thickness of approximately 200–300 nm, is found in Fig. 4 (Bottom Left). Here too only one p-polarized emission peak was observed and the angle was at 308° (or 52°). It is obvious that the SPCE is exclusively p-polarized light. The intensity of the SPCE was compared with the free space intensity at 230°. The ratio is found to be 2.0. For sample D, where 482 nm silica nanoparticles were used and had an estimated average film thickness of approximately 300 nm, it is interesting to note that the p-polarized SPCE was again observed at 308° (or 52°) as shown in Fig. 4 (Bottom Right). However, the intensity of SPCE is much weaker in comparison with the free space intensity. The ratio is reduced to 0.35. The change in the surface topography of the dielectric coating definitely affects the out-coupling efficiency of light emission.
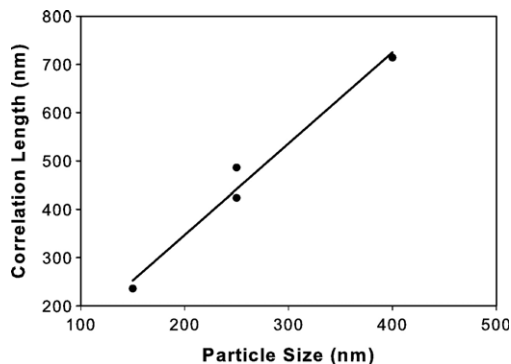
It is interesting to note though that the surface roughness has, for the most part, not affected the angular distribution of the SPCE.

The surface morphology of similar randomly roughened silica coating has been studied extensively by AFM in a previous patent [28]. The height image of sample B is shown in Fig. 5. The average roughness (Sa) and root mean square average roughness (Sq) can be known from the 5×5 µm image and equal to 20 and 27 nm, respectively. In addition, the degree of roughness was determined by using fast Fourier transform of the 2D height image and correlated with the correlation length of pair correlation function. The pair correlation function $g(r_1,r_2)$ is defined as, given a particle at position r_1, the probability of finding a second particle at position r_2. Depending on the packing density, $g(r_1,r_2)$ will show structure features in the short range and gradually levels off to a constant at larger distances. The distance it showed structure represents the correlation length. When a system has a crystal like structure, this range extends to infinity (or the size of the crystal domain). This is normally called long-range ordering. A regular photonic structure is composed of particles with periodical structures of a length scale comparable to wavelength and extend to very long-range ordering. We believe our structure has only short-range ordering. Results obtained from studying a series of coating samples and disclosed in a previous patent established a linear relationship between the surface correlation length and the particle size, shown in Fig. 6 [28]. The empirical equation is as follows:

$$L = 1.83 * X - 20 \qquad (1)$$

where L is the surface correlation length determined by AFM along with Fourier transform, X is the silica nanoparticle size measured by dynamic light scattering. According to this equation the surface correlation length scales L for samples A, B, C and D in this paper would be 2 nm, 255 nm, 584 nm and 862 nm, respectively. The linear relationship between average surface roughness and the particle size is summarized in Fig. 7.

For sample A, with a film thickness of approximately 316 nm and minimal surface roughness (the sample can almost be regarded as a smooth surface), the waveguide modes of SPCE are predominant. Hence different waveguide modes can be observed at various angles with alternating s and p polarizations. Sample B having a film thickness of approximately 120 nm does
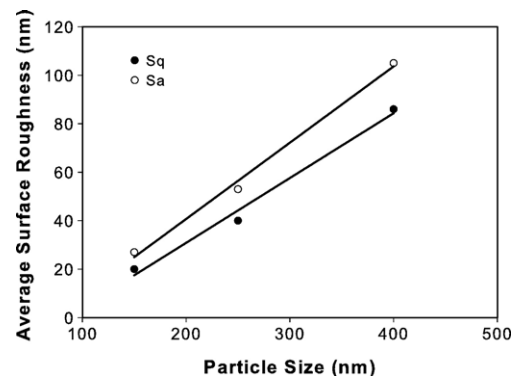

Fig. 6. Linear relationship between silica nanoparticles and correlation distance of the coating surface topography [$L=1.83 \times -20$ (nm)].

Fig. 7. Linear relationship between average surface roughness (Sa and Sq) of the coating surface Vs size of silica nanoparticles.

not fall in the waveguide regime and hence we do not see multiple peaks. Although sample C with a film thickness of approximately 200–300 nm, and sample D with a film thickness of approximately 300 nm fall into the waveguide regime, the waveguide mode of SPCE is significantly suppressed with the increase in the surface roughness. Only one peak with p polarization can be observed and the angle is consistently appeared at 308° (or 52°). These results indicate that surface roughness plays a role in waveguide mode suppression, the exact mechanism of which is not entirely clear at this point.

The enhancement of the SPR coupled emission may originate from three different phenomena: (a) Enhancement of dye emission, (b) Enhancement of SPR coupling, (c) Enhancement of light extraction from SPR. Our coating is composed of fluorinated silica particles of a definite size. Because of the fluorination, the refractive index of the particle can be lowered below that of the dye resin mixture. When the particle size is near the wavelength scale, the differences in refractive indexes resulted in effects resembling those of a photonic structure i.e. a composite structure with a periodic variation in dielectric constant of a length scale in the optical wavelength range [29]. Light may be reflected among wavelength scale particles and enhance the local EM field around the dye molecules. This can amplify the emission of the dye molecules. In addition, this variation in dielectric constants at this wavelength scale could enhance the light coupling in with the SPR modes in the metal. Furthermore, a periodic variation of dielectric constants (such as a grating structure) near the interface of a thin metal film is also known to substantially increase the rate of release of energy in the form of far field radiation that would have otherwise have been coupled within bound surface optical modes (such as SPP modes and waveguide modes), and unable to radiate [3–9].

The amplifications in dye emission may have originated from the spontaneous and/or stimulated (induced) energy transfers among two quantum states. The induced emission is amplified by increased field density while the spontaneous emission is amplified by mode coupling with the metal SPR which has a high mode density in the visible spectrum domain. The mechanisms of coupling in and coupling out with SPR by having periodical dielectric contrast at a distance and correlation length scale corresponding to the relevant wavelength are essential for the enhancements of the spontaneous emission.

Strictly speaking, our coating layers, although containing periodical variations in the dielectric constant does not constitute a photonic material of conventional definition. The ordering structure in our coating is only short-ranged, while a regular photonic material has a long-range ordering [30]. For our coating, when using a high concentration of particles, the volume exclusion effects leads to a pair correlation function peaking at a distance determined by the particle diameter. This would lead to a short-ranged photonic structure at a length scale set by the particle size. Furthermore, the fluorinated particles, having a very low surface free energy due to the fluorine atoms, tend to accumulate at the resin–air interface, leading to a dense and, consequently, a higher ordering structure at the interface. The experiments to quantify each mode of enhancement contributions are still underway and their results will be reported

in due course. At present, the optimized coating formulation (i.e. the particle size, fluorine content and correlation length) regarding SPCE enhancement are determined empirically.

4. Conclusions

Conventional OLEDs consist of a transparent conductive anode and an opaque (Al or Ag) electrode on top. The emitted light must come out through the bottom anode, making the 'on-chip' OLED integration with silicon driver electronics rather difficult. A device capable of emitting light from the top cathode would allow all circuitry components such as wiring and transistor to be placed at the bottom and not interfering with light output. Therefore, there has been an increasing demand in TOLED for active-matrix OLED display. The results discussed in this paper suggest that SPCE can enhance the light emission and transmission through a thin silver layer and thus be integrated with the design of a top Ag electrode in TOLEDs.

Recent advancements in LED lighting technology also cited the use of roughened metal films to enhance quantum yields of many fluorophores [1,31,32]. Thus, it is an indication that, by incorporating the roughened metal films with SPCE, the lighting efficiency of LED could also be substantially increased. Given that we have previously shown the feasibility of surface plasmon-coupled electroluminescence on thin gold films, we expect an expansion of this technique from photoluminescence to electroluminescence will extend the applications of coating-enhanced SPCE from LCD displays to OLED, LED and field emission devices [33].

The light emission enhancements by SPCE have a broad impact in optical displaying technologies. By separating a polarization and/or colors, part of the light energy can be recycled to increase the power efficiency. However, the scheme outlined here goes a step further by guiding the returned light back in a photonic cavity to accomplish higher stimulated emission [34,35]. The presence of metal surfaces at sub-micron dimensions may enhance spontaneous emission as well. These technologies are important to the design of a backlight source in future LCD panels where the light use efficiency is critical to their performances [36].

Acknowledgements

References

[1] K. Okamoto, I. Niki, A. Shvartser, Y. Narukawa, T. Mukai, A. Scherer, Nat. Mater. 3 (2004) 601.
[2] D.K. Gifford, D.G. Hall, Appl. Phys. Lett. 80 (2002) 3679.
[3] L.H. Smith, J.A.E. Wasey, W.L. Barnes, Appl. Phys. Lett. 84 (16) (2004) 2986.

[4] P.A. Hobson, S. Wedge, J.A.E. Wasey, I. Sage, W.L. Barnes, Adv. Mater. 14 (19) (2002) 1393.

[5] W.L. Barnes, J. Mod. Opt. 45 (4) (1998) 661.

[6] J.M. Lupton, B.J. Matterson, I.D.W. Samuel, M.J. Jory, W.L. Barnes, Appl. Phys. Lett. 77 (21) (2000) 3340.

[7] R. Windisch, P. Heremans, A. Knobloch, P. Kiesel, G.H. Döhler, B. Dutta, G. Borghs, Appl. Phys. Lett. 74 (16) (1999) 2256.

[8] I. Schnitzer, E. Yablonovitch, C. Caneau, T.J. Gmitter, A. Scherer, Appl. Phys. Lett. 63 (16) (1993) 2174.

[9] T. Tsutsui, M. Yahiro, H. Yokogawa, K. Kawano, M. Yokoyama, Adv. Mater. 13 (15) (2001) 1149.

[10] J.R. Lakowicz, Principles of Fluorescence Spectroscopy, Springer, New York, 2006.

[11] J.R. Lakowicz, Anal. Biochem. 298 (2001) 1.

[12] J.R. Lakowicz, Anal. Biochem. 301 (2002) 261.

[13] J.R. Lakowicz, Anal. Biochem. 324 (2004) 153.

[14] I. Gryczynski, J. Malicka, Z. Gryczynski, J.R. Lakowicz, Anal. Biochem. 324 (2004) 170.

[15] C.D. Geddes, K. Aslan, I. Gryczynski, J. Malicka, J.R. Lakowicz, in: C.D. Geddes, J.R. Lakowicz (Eds.), Annual Reviews in Fluorescence, Kluwer Academic/Plenum, New York, 2004, p. 365.

[16] K. Aslan, Z. Leonenko, J.R. Lakowicz, C.D. Geddes, J. Fluoresc. 15 (5) (2005) 643.

[17] J.R. Lakowicz, Anal. Biochem. 337 (2005) 171.

[18] I. Gryczynski, J. Malicka, K. Nowaczyk, Z. Gryczynski, J.R. Lakowicz, J. Phys. Chem., B 108 (2004) 12073.

[19] I. Gryczynski, J. Malicka, Z. Gryczynski, J.R. Lakowicz, J. Phys. Chem., B 108 (2004) 12568.

[20] C.D. Geddes, I. Gryczynski, J. Malicka, Z. Gryczynski, J.R. Lakowicz, J. Fluoresc. 14 (2004) 119.

[21] I. Gryczynski, J. Malicka, Z. Gryczynski, K. Nowaczyk, J.R. Lakowicz, Anal. Chem. 76 (2004) 4076.

[22] E. Matveeva, Z. Gryczynski, I. Gryczynski, J. Malicka, J.R. Lakowicz, Anal. Chem. 76 (2004) 6287.

[23] I. Gryczynski, J. Malicka, W. Jiang, H. Fischer, W.C.W. Chan, Z. Gryczynski, W. Grudzinski, J.R. Lakowicz, J. Phys. Chem., B 109 (2005) 1088.

[24] I. Gryczynski, J. Malicka, K. Nowaczyk, Z. Gryczynski, J.R. Lakowicz, Thin Solid Films 510 (2006) 15.

[25] A.J.M. Yang, R. Zhang, US Patent Application, Pub. No. 2006/0074172, April 6, 2006.

[26] W. Stöber, A. Fink, E. Bohn, J. Colloid Interface Sci. 26 (1968) 62.

[27] K. Lee, A.N. Sathyagal, A.V. McCormick, Colloids Surf., A Physicochem. Eng. Asp. 144 (1998) 115.

[28] X. Wu, R. Zhang, A.J.M. Yang, US Patent Application 60/656097, 2005.

[29] J.D. Joannopoulos, R.D. Meade, J.N. Winn, Photonic Crystals—Molding the Flow of Light, Princeton University Press, New Jersey, 1995.

[30] J.D. Joannopoulos, P.R. Villeneuve, S. Fan, Nature 386 (1997) 143.

[31] T. Fujii, Y. Gao, R. Sharma, E.L. Hu, S.P. DenBaars, S. Nakamura, Appl. Phys. Lett. 84 (2004) 855.

[32] K. Okamoto, I. Niki, A. Scherer, Y. Narukawa, T. Mukai, Y. Kawakami, Appl. Phys. Lett. 87 (2005) 071102.

[33] J. Zhang, Z. Gryczynski, J.R. Lakowicz, Chem. Phys. Lett. 393 (2004) 483.

[34] C. Hui, J. Phys. A: Math. Gen. 38 (2005) 10497.

[35] Y. Feng, K. Ueda, Phys. Rev., A 68 (2003) 025803.

[36] A.J.M. Yang, X. Wu, R. Zhang, US Provisional Patent Application ref. no. 121747-06085637, 5 July 2006.